EUROPEAN ORGANIZATION FOR NUCLEAR RESEARCH

Proposal to the ISOLDE and Neutron Time-of-Flight Committee

# Coulomb Excitation of Neutron-rich $^{134,136}$Sn isotopes

October 3, 2012

Th. Kröll[1], M. Scheck[1], S. Bönig[1], M. Thürauf[1], S. Ilieva[1], M. von Schmid[1], J. C. Zamora[1], A. Ignatov[1], A.-L. Hartig[1], C. Henrich[1], C. Bauer[1], R. Stegmann[1], N. Pietralla[1], C. Stahl[1], G. Simpson[2], M. Ramdhane[2], G. Gey[2], F. Drouet[2], U. Köster[16], R. Krücken[3,4], R. Gernhäuser[3], D. Mücher[3], K. Nowak[3], P. Thirolf[5], M. Huyse[6], K. Wrzosek-Lipska[6], N. Kesteloot[6], P. Van Duppen[6], R. Orlandi[6], F. Wenander[7], D. Voulot[7], T. Stora[7], E. Rapisarda[7], A. Jungclaus[8], A. Illana Sisón[8], G. Rainovski[9], K. Gladnishki[9], M. Danchev[9], D. Bucurescu[10], N. Mărginean[10], R. Mărginean[10], D. Deleanu[10], A. Negret[10], D. Balabanski[11], K. Hadynska-Klek[12], N. Warr[13], A. Blazhev[13], P. Reiter[13], B. Siebeck[13], M. Seidlitz[13], K. Wimmer[14], V. Bildstein[15], R. Chapman[17], G. Georgiev[18], T. Grahn[19,20], P. T. Greenlees[19,20], J. Pakarinen[19,20], P. Rahkila[19,20], R. Lozeva[21], J. Cederkäll[22], A. Andreyev[23], L. M. Fraile[24], and the MINIBALL and HIE-ISOLDE collaborations

[1] *TU Darmstadt, Germany*; [2] *LPSC, Grenoble, France*; [3] *TU München, Germany*; [4] *TRIUMF, Vancouver, Canada*; [5] *LMU München, Germany*; [6] *KU Leuven, Belgium*; [7] *CERN, Genève, Switzerland*; [8] *IEM CSIC, Madrid, Spain*; [9] *Univ. of Sofia, Bulgaria*; [10] *IFIN-HH, Bucharest, Romania*; [11] *INRNE-BAS, Sofia, Bulgaria*; [12] *Uniw. Warszawski, Poland*; [13] *Univ. zu Köln, Germany*; [14] *Central Michigan University, Mt. Pleasant MI, USA*; [15] *Univ. of Guelph, Canada*; [16] *ILL, Grenoble, France*; [17] *Univ. West of Scotland, Paisley, UK*; [18] *CSNSM, Orsay, France*; [19] *Univ. of Jyväskylä, Finland*; [20] *Helsinki Institute of Physics, Finland*; [21] *IPHC, Strasbourg, France*; [22] *Lunds Univ., Sweden*; [23] *Univ. of York, UK*; [24] *UC Madrid, Spain*

**Spokespersons:** Th. Kröll [tkroell@ikp.tu-darmstadt.de], G. Simpson [simpson@lpsc.in2p3.fr]
**Contact person:** E. Rapisarda [elisa.rapisarda@cern.ch]

CERN-INTC-2012-042 / INTC-P-343
03/10/2012

**Abstract:** We propose to study excited states in the isotopes $^{134,136}$Sn by $\gamma$-ray spectroscopy following "safe" Coulomb excitation. The experiment aims to investigate the evolution of quadrupole collectivity beyond the magic shell closure at $N = 82$ by the determination of $B(E2)$ values and electric quadrupole moments $Q_2$. Recent shell-model calculations using realistic interactions predict possible enhanced collectivity in neutron-rich regions. Evidence for this could be obtained by this experiment. Furthermore, the currently unknown excitation energies of the $2_1^+$ and $4_1^+$ states in $^{136}$Sn will be measured for the first time.

**Requested shifts:** [30] shifts, (split into [1] runs over [1] years)

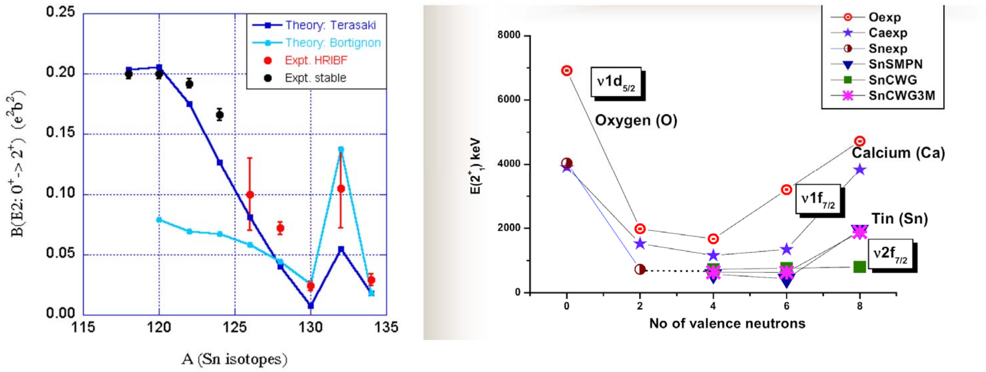


Figure 1: *Experimental* $B(E2; 0^+_{gs} \rightarrow 2^+)$ *values compared to QRPA calculations [6] (left) and excitation energies* $E(2^+)$ *compared to shell-model calculations [12] (right).*

# 1 Physics case

The region around the doubly-magic nucleus $^{132}$Sn is the focus of many efforts in both experimental and theoretical nuclear physics. This is because it is one of only two doubly magic, medium-heavy, neutron-rich regions which are currently experimentally accessible, the second region being that around $^{78}$Ni. Since the astrophysical $r$ process is expected to pass through this region, the understanding of the nuclear structure has also an impact on the description of the $A \approx 130$ peak in the solar element abundances. The programme sketched in our LoI which has been endorsed by the INTC in 2010 aims for investigation of nuclear structure in this region [1].

The Sn isotopes between $^{102}$Sn and $^{130}$Sn are almost perfect textbook examples of nuclei described by a seniority scheme. The excitation energy of the first $2^+$ state is nearly constant at around 1200 keV and the $B(E2; 0^+_{gs} \rightarrow 2^+)$ values show a parabolic behaviour peaking at mid-shell. However, starting around mid-shell from $^{114}$Sn for the neutron-deficient isotopes, an enhancement of quadrupole collectivity has been observed, see for example [2, 3, 4]. A weakening of the closure at $Z = 50$ has been suggested as possible explantion. On the other hand, the GT strength observed in the $\beta$-decay of $^{100}$Sn has proven the simultaneous robustness of both shell closures at $Z = 50$ and $N = 50$ in this doubly-magic nucleus [5].

Interestingly, the picture changes dramatically going beyond $N = 82$. The excitation energy of the first $2^+$ state in $^{134}$Sn is only at 725.6 keV. In contrast, the recently measured $B(E2; 0^+_{gs} \rightarrow 2^+)$ value of 0.029(5) $e^2$b$^2$ value is very similar to the value for the two-hole nucleus $^{130}$Sn [6]. However, the value has a large error as it has been determined from a $\gamma$-ray spectrum obtained with low-resolution $BaF_2$ detectors.

Various approaches have been used to generate shell-model interactions capable of prediciting the behavior of neutron-rich nuclei beyond $N = 82$ using either empirical approaches (e.g. SMPN) [9] or realistic free nucleon-nucleon potentials (e.g. CD-Bonn), renormalized by either G-matrix (e.g. CWG) [10] or $V_{low\,k}$ methods [8]. Despite the fact that the $B(E2; 0^+_{gs} \rightarrow 2^+)$ value for $^{134}$Sn is nicely reproduced, the predictions for $^{136}$Sn, and beyond, differ considerably. Whereas the calculations with empirical interactions predicts even a new shell closure at $N = 90$ as the $\nu f_{7/2}$ orbital is filled, the calculations with realistic interactions do not find such an effect. As it can be seen in Table 1, already for $^{136}$Sn the predictions for the $E(2^+)$ excitation energies differ by 150 keV and for the $B(E2; 0^+_{gs} \rightarrow 2^+)$ value by nearly 40%.

| | $^{134}$Sn | | $^{136}$Sn | $^{138}$Sn |
|---|---|---|---|---|
| | exp. | theo. | theo. | theo. |
| $E(2^+)$ [keV] | 726.5 [13] | 774.8 [10]<br>733.0 [9] | 733.9 [10]<br>578.0 [9]<br>639.0 [12] | 761.5 [10]<br>433.0 [9]<br>633.0 [12] |
| $E(4^+)$ [keV] | 1073.4 [13] | 1116.1 [10]<br>1070.0 [9] | 1161.4 [10]<br>884.0 [9] | 1355.0 [10]<br>736.0 [9] |
| $E(6^+)$ [keV] | 1247.4 [13] | 1258.2 [10] | 1377.0 [10] | 1528.8 [10] |
| $B(E2; 0^+_{\rm gs} \rightarrow 2^+)$ [$e^2$b$^2$] | 0.029(5) [6] | 0.031 [10]<br>0.029 [9]<br>0.034 [8] | 0.062 [10]<br>0.045 [9] | 0.089 [10]<br>0.034 [9] |
| $B(E2; 2^+ \rightarrow 4^+)$ [$e^2$b$^2$] | | 0.031 [10]<br>0.034 [8] | 0.043 [10] | $2 \cdot 10^{-4}$ [10] |
| $B(E2; 4^+ \rightarrow 6^+)$ [$e^2$b$^2$] | 0.0182(35) [7] | 0.017 [10]<br>0.017 [8] | 0.007 [10] | 0.006 [10] |

Table 1: Experimental properties and predictions by shell-model calculations for the neutron-rich even Sn isotopes beyond $N = 82$.

Beyond these specific measurements, knowledge of the structure of the Sn isotopes is particularly important test to test the neutron-neutron part of shell-model interactions as proton-proton and proton-neutron terms do not contribute at low energies and, therefore, low-lying states have a pure neutronic character. The results of the proposed experiment will aid the understanding of the evolution of neutron-neutron two-body matrix elements in nuclei with large neutron excesses.

The $\nu f_{7/2}$ orbit, present at low energies in the Sn nuclei beyond $N = 82$ has an interesting analogy with the situation in the Ca isotopic chain where a $\nu f_{7/2}$ orbital is filled between $N = 20$ and $N = 28$. There was the long-standing problem that realistic interactions were not able to reproduce the shell closure at $N = 28$. This has been resolved very recently by including three-body forces [11]. Indeed, including three-body forces a shell closure at $N = 90$ occuring in $^{140}$Sn is predicted also by calculations based on realistic interactions (CWG3M) [12] (Fig. 1, right).

The Sn isotopes around $^{132}$Sn have been also discussed in the framework of a reduced neutron pairing gap above $N = 82$. However, it has been found that, as expected, the $B(E2)$ value is rather insensitive, whereas the low excitation energy is better reproduced in QRPA calculations assuming a weaker neutron pairing [14]. Fig. 1 (left) shows the experimental $B(E2; 0^+_{\rm gs} \rightarrow 2^+)$ values compared to QRPA calculations.

For $^{136}$Sn, not even the excitation energy of the first $2^+$ state is known yet. It has to be mentioned that there are ongoing attempts to measure this value at RIKEN in secondary fragmentation. The excitation energies in $^{136,138}$Sn may also be measured in an upcoming isomer spectroscopy experiment with the EURICA spectrometer at RIKEN, aiming to observed the delayed decay of the $6^+$ isomers with dominant $\nu f^2_{7/2}$ configurations, the analogues to the isomeric $6^+$ state in $^{134}$Sn ($T_{1/2} = 80(15)$ ns) [7]. So, the values of the excitation energies may be known when the proposed experiment will be performed.

We propose to measure the $B(E2; 0^+_{\rm gs} \rightarrow 2^+)$ values for the neutron-rich isotopes $^{134,136}$Sn. For $^{134}$Sn the precision will be improved and for $^{136}$Sn it will be the first determination. For both nuclei, the $B(E2; 2^+ \rightarrow 4^+)$ will be measured first time. Also electric quadrupole moments $Q_2$ can be extracted from the experimental data. Additionally, the excitation energy of the first $2^+$ and $4^+$ states in $^{136}$Sn will be measured.

# 2 Experimental method and set-up

We will apply the method of $\gamma$-ray spectroscopy following "safe" Coulomb excitation. The set-up will consist of the MINIBALL Ge array and a Si detector array. For the proposed experiment, the advantage of HIE-ISOLDE compared to REX-ISOLDE is the increased probability for multi-step processes due to the higher beam energy and the use of a heavy target. This enables to us study also the $4^+$ state.
The excitation cross section for Coulomb excitation depends not only on the transitional but also on the diagonal matrix elements, an effect known as reorientation. As both the relative importance of single- and multi-step processes and the reorientation effect depend on the scattering angle, a data set with a large coverage of scattering angles in the CM system is mandatory. In the analysis, the data set is split in different angular bins. The matrix elements are then determined by a maximum likelihood fit.
The analysis of the excitation cross section will be performed relative to the excitation of the target. We intend to use a lead target to maximise the excitation cross section. Excited states in the doubly-magic $^{208}$Pb, if at all, will only hardly be populated. The isotope $^{206}$Pb ($E(2^+) = 803$ keV) is well suited as the nearest $\gamma$-ray from $^{134}$Sn is at 725.6 keV. The excitation energies in $^{136}$Sn are not known yet, but all predictions from theory result in $\gamma$-ray energies below 750 keV. The less abundant $^{204}$Pb ($E(2^+) = 899$ keV, $E(4^+) = 1274$ keV) could be used too although its ($4^+ \rightarrow 2^+$)-transition may overlap with transitions from $^{136}$Sn. The $3^-$ states are above 2.6 MeV for both Pb isotopes and decay by high-energy $\gamma$-rays.
As Si detector to detect the particles we consider either the standard CD DSSSD detector or a modified version of T-REX [22]. For the latter, the forward barrel would be removed and the forward CD placed at the same distance to the target as the standard CD. The advantage would be that the optimal angular coverage (in the CM system) of the CD is retained, but additional coverage in backward direction by the backward barrel is added. The backward CD is not used.
However, it has to mentioned that the efficiency of MINIBALL using T-REX is somewhat smaller compared to the standard CD scattering chamber because of the larger distances of the MINIBALL detectors to the target. Given the expected rates, see below, this is not an important drawback.
The "safe" energy for $^{134,136}$Sn on lead is about 4.4 MeV/u ($\vartheta_{\mathrm{CM}} = 180°$) applying a well-established empirical formula suited for such heavy scattering systems [21].
In Fig. 2, the expected energies of the scattered projectiles and the recoiling target nuclei are shown. The energy loss in the target was interpolated using some nodes calculated with SRIM2008 [19]. The pulse height deficit was included too using the simple

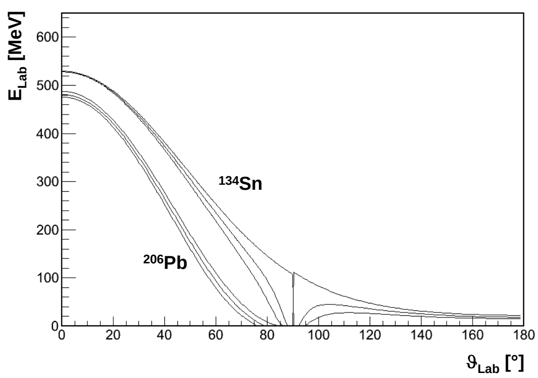


Figure 2: *Kinetic energies of scattered $^{134}$Sn projectiles and recoiling $^{206}$Pb target nuclei for an incident energy of 4.4 MeV/u and a target thickness of 1 mg/cm$^2$. The lines show the limiting cases of a scattering at the front, the middle, or the back layers of the target, respectively.*

model from Ref. [20] (neglecting the small detector dependent term). It can be seen that the projectiles and the recoils are well separated below $\vartheta > 70°$. The use of a target thicker than 1 mg/cm$^2$ would reduce the separation considerably. The beam energy at the middle of the target will be 573 MeV (4.27 MeV/u) and 581 MeV (4.28 MeV/u) for $^{134,136}$Sn, respectively. Table 2 summarises the calculated cross sections for elastic scattering and the excitation of the first three states in $^{134,136}$Sn. The matrix elements, and for $^{136}$Sn also the excitation energies, are taken from Ref. [10]. The different sensitivities on single- or multi-step excitation at different scattering angles, e.g. the ratio $\sigma(6^+)/\sigma(2^+)$, are obvious. In order to illustrate the reorientation effect, the cross sections have been calculated assuming the same diagonal maxtrix element of 0 $e$b and $\pm 0.5$ $e$b for all states resulting in changes in the cross section by up to 40 %, in particular at backward angles. This demonstrates the advantage of the larger angular coverage using T-REX. The diagonal matrix elements may be expected to be small, e.g. in $^{124,126,128}$Sn values compatible with zero have been found [18]. However, for $^{134}$Sn a quite large $Q_2(2_1^+) = 1.6$ $e$b is predicted [8]. The cross section for the target excitation is in the order of 0.5 b.
As it can be seen from Table 2, we expect that only the $2_1^+$ and $4_1^+$ states will be excited. Hence, the analysis described above has to consider only two transitional and two diagonal matrix elements. The analysis will not be affected by the $6^+$ state, as its excitation probability, if compared to the $4^+$ state, is more than two orders of magnitude smaller. Finally, in contrast to multiple Coulomb excitation of more collective nuclei no additional constraints from other experiments, like lifetimes, are required in order to simplify the analysis.
The short-lived isotope $^{136}$Sn ($T_{1/2} = 250$ ms [13]) will partially decay in REX-TRAP and REX-EBIS causing an unvoidable beam contamination. However, the situation is very similar to $^{128}$Cd ($T_{1/2} = 300$ ms) successfully measured in 2011 (IS477). The half-life is slightly shorter, but we start with a clean beam without any Cs contamination unlike for Cd. The isotope $^{134}$Sn ($T_{1/2} = 1.06$ ms [13])will decay only to a small amount, about 10 %, similar to $^{142}$Xe (1.23 s) measured during one of the IS411 campaigns [16].
The beam composition will be determined from the characteristic $\gamma$-rays from the decay of the Sn and Sb isotopes. The longest half-live involved is 10.1 s, hence no long activation times are required. For this, the beam will be stopped occasionally at the target position within MINIBALL as it has been done e.g. in experiment IS477 for Cd beams [17].

# 3 Rate estimate and beam time request

The Sn isotopes are produced with a standard UC$_x$/graphite target irradiated with the proton beam from the PS Booster. In order to eliminate the Cs contamination, we will extract SnS$^+$ molecules which will be cracked afterwards in the EBIS. Natural sulphur which contains the isotopes $^{32,33,34,36}$S (94%, 0.75%, 4.2%, 0.02%). To produce e.g. $^{136}$Sn, a $A = 168$ beam would contain $^{136}$Sn$^{32}$S$^+$ but also a strong contamination from the more more abundant Sn isotope, hence $^{134}$Sn$^{34}$S$^+$. Therefore, we will use isotopically enriched $^{34}$S and produce a very clean $A = 170$ beam containing only $^{136}$Sn$^{34}$S$^+$ molecules [23].
Recent developments of the ISOLDE target group with the VD5 ion source enable higher yields compared to Ref. [23]. We expect yields of $10^6/\mu$C and $2 \cdot 10^4/\mu$C for $^{134,136}$Sn, respectively [24]. Currently, $^{138}$Sn is out of reach for ISOLDE.
The isotopes $^{134,136}$Sn decay subsequently to their respective stable Xe isobars. The decay products involved with longest half-lifes are $^{134}$I (52 min) and $^{134}$Te (41.8 min). Therefore, activation by long-lived decay products is no issue for the experiment and radiation

| | $15° < \vartheta_{\mathrm{Lab},3} < 50°$ ($25° < \vartheta_{\mathrm{CM}} < 80°$) | $15° < \vartheta_{\mathrm{Lab},4} < 50°$ ($80° < \vartheta_{\mathrm{CM}} < 150°$) | $105° < \vartheta_{\mathrm{Lab},3} < 153°$ ($145° < \vartheta_{\mathrm{CM}} < 170°$) |
|---|---|---|---|
| Ruth | 43 | 3 | 0.2 |
| $^{134}$Sn: $2^+$ | 0.40(3) | 0.32(8) | 0.039(16) |
| $4^+$ | 0.0026(2) | 0.010(2) | 0.0020(6) |
| $6^+$ | $5.3 \cdot 10^{-6}$ | $7.9 \cdot 10^{-5}$ | $2.5 \cdot 10^{-5}$ |
| $^{136}$Sn: $2^+$ | 0.80(8) | 0.80() | 0.065(29) |
| $4^+$ | 0.0073(7) | 0.025(5) | 0.0047(13) |
| $6^+$ | $6.7 \cdot 10^{-6}$ | $8.7 \cdot 10^{-5}$ | $2.5 \cdot 10^{-5}$ |

Table 2: *Calculated cross sections, in [b], for a $^{134}$Sn ($^{136}$Sn) beam at 573 MeV (581 MeV) on a lead target. The variation due to the reorientation effect is given in parenthesis (see text).*

protection.

Assuming a proton current of 2 $\mu$A and, conservatively, an efficiency of HIE-ISOLDE of 5% the expected beam intensities will be $10^5$/s and $2 \cdot 10^3$/s. Because of decay losses in the EBIS, we assume in the following an intensity of $10^3$/s for the short-lived $^{136}$Sn . We require the slow extraction from the EBIS to reduce the instantaneous particle rate. Taking into account the cross sections from Table 2, the count rate of the particle detectors will be 13/s corresponding to about 13 kHz within the pulse (assumed pulse length 200 $\mu$s and an EBIS rate of 5 Hz) which is easily handable.

The CD detector is divided in 2.5° bins (annular strips). Hence, the obtained statistics should allow to split the data set in 5-12 angular bins. Reasonably, the forward CD can be divided in 10 angular bins (5 for the scattered projectiles and 5 for the recoiling target nuclei) corresponding to 3-4 annular strips per bin and covering in average 9° each. For lower statistics, only 4 bins are considered covering 17.5° each. The backward barrel collects less than 10 % of the total statistics, so it will be split in two bins or taken as one single bin.

The deorientation effect on the measured $\gamma$-ray yields in MINIBALL, not included in the following estimates, is very small and can be extracted from the data [16].

The $\gamma$-particle coincidence rates will be 750/h and 13/h for the decay of the $2^+$ and $4^+$ states in $^{134}$Sn, respectively. The error of the $B(E2; 0^+_{\mathrm{gs}} \rightarrow 2^+)$ value of the previous experiment is 17 % [6]. We aim to improve this error to below 5 %. As already mentioned, the impact of the diagonal matrix elements (not discussed in [6]) is expected to be small.

In order to obtain an average statistical error of 2 % per angular bin (9°), 2 days of beam time are required. If the backward barrel is split into two bins a statistical error of about 3 % for each is obtained. In order to have a statistical error below 10 % for 4 angular bins in the CD for the $4^+$ state, 500 counts are needed. The $B(E2; 2^+_{\mathrm{gs}} \rightarrow 4^+)$ and, possibly, the electric quadrupol moments $Q_2$ for both states will be determined for the first time. We require **2 days (6 shifts) of beam time for $^{134}$Sn**.

The $\gamma$-particle coincidence rates will be 16/h and 0.3/h for the decay of the $2^+$ and $4^+$ states in $^{136}$Sn, respectively. Within a beam time of 8 days, 3000 (50) counts in total will be collected for the $2^+$ ($4^+$) state. This allows to study the $2^+$ state in detail by splitting the data set into 4 angular bins with an average statistical error below 5 % for each of them. The predictions from the different shell-model calculations differ by nearly 40 %. In order to allow a distinction between them, a total error below 10 % is envisaged. The backward barrel will be taken as one single bin (statistical error < 10 %). The $B(E2; 2^+_{\mathrm{gs}} \rightarrow 4^+)$ value will be obtained within a precision of about 20 % as the statistics obtained do not allow a splitting of the data set. It should be remembered that, so far, not even the excitation energies of the states in $^{136}$Sn are known! We require **8 days (24 shifts) of beam time for $^{136}$Sn**.

**Summary of requested shifts:**
**In total, we request 10 days (30 shifts) of beam time for $^{134,136}$Sn**.

# References


[1] Th. Kröll et al., CERN-INTC-2010-045 / INTC-I-111.

[2] J. Cederkäll et al., Phys. Rev. Lett. 98, 172501 (2007).

[3] A. Ekström et al., Phys. Rev. Lett. 101, 012502 (2008).

[4] P. Doornenbal et al., Phys. Rev. C 78, 031303(C) (2008).

[5] C. B. Hinke et al., Nature 486, 341 (2012).

[6] R. L. Varner et al., Eur. Phys. J. A 25, s01, 391 (2005).

[7] A. Korgul et al., Eur. Phys. J. A 7, 167 (2000).

[8] A. Covello et al., J. Phys.: Conf. Ser. 267, 012019 (2011).

[9] S. Sarkar and M. Saha Sarkar, Phys. Rev. C 78, 024308 (2008).

[10] M. P. Kartamyshev et al., Phys. Rev. C 76, 024313 (2007).

[11] J. D. Holt et al., J. Phys. G: Nucl. Part. Phys. 39, 085111 (2012).

[12] S. Sarkar and M. Saha Sarkar, J. Phys.: Conf. Ser. 267, 012040 (2011).

[13] `http://www.nndc.bnl.gov`

[14] J. Terasaki Phy. Rev. C 66, 054313 (2002).

[15] G. Colò et al., Nucl. Phys. A 722, 111c (2003).

[16] T. Behrens, PhD Thesis (TU München, 2010); publication in preparation.

[17] S. Bönig, ISOLDE Workshop; PhD Thesis (TU Darmstadt, expected for 2013).

[18] J. M. Allmond et al., Phys. Rev. C 84, 061303(R) (2011).

[19] J. F. Ziegler, `http://www.srim.org`

[20] G. Pasquali et al., Nucl. Instr. Meth. A 405, 39 (1998).

[21] H. J. Wollersheim, Habilitation Treatise (Universität Frankfurt/M, 1993).

[22] V. Bildstein et al., Eur. Phys. J. A 48, 85 (2012).

[23] U. Koester et al., Nucl. Instr, Meth. B 266, 4229 (2008).

[24] T. Stora, private communication.

# Appendix

**DESCRIPTION OF THE PROPOSED EXPERIMENT**

The experimental setup comprises: (*MINIBALL + T-REX*)

| Part of the | Availability | Design and manufacturing |
|---|---|---|
| (if relevant, name fixed ISOLDE installation: [MINIBALL + T-REX] | ☒ Existing | ☒ To be used without any modification |
| [MINIBALL] | ☒ Existing | ☒ To be used without any modification<br>☐ To be modified |
| | ☐ New | ☐ Standard equipment supplied by a manufacturer<br>☐ CERN/collaboration responsible for the design and/or manufacturing |
| [CD] | ☒ Existing | ☒ To be used without any modification<br>☐ To be modified |
| | ☐ New | ☐ Standard equipment supplied by a manufacturer<br>☐ CERN/collaboration responsible for the design and/or manufacturing |
| [insert lines if needed] | | |

HAZARDS GENERATED BY THE EXPERIMENT (if using fixed installation:) Hazards named in the document relevant for the fixed [MINIBALL + T-REX] installation.

Additional hazards:

| Hazards | [Part 1 of experiment/ equipment] | [Part 2 of experiment/ equipment] | [Part 3 of experiment/ equipment] |
|---|---|---|---|
| **Thermodynamic and fluidic** | | | |
| Pressure | [pressure][Bar], [volume][l] | | |
| Vacuum | | | |
| Temperature | [temperature] [K] | | |
| Heat transfer | | | |
| Thermal properties of materials | | | |
| Cryogenic fluid | [fluid], [pressure][Bar], [volume][l] | | |
| **Electrical and electromagnetic** | | | |
| Electricity | [voltage] [V], [current][A] | | |
| Static electricity | | | |
| Magnetic field | [magnetic field] [T] | | |
| Batteries | ☐ | | |
| Capacitors | ☐ | | |
| **Ionizing radiation** | | | |

| | | | |
|---|---|---|---|
| Target material [material] | | | |
| Beam particle type (e, p, ions, etc) | | | |
| Beam intensity | | | |
| Beam energy | | | |
| Cooling liquids | [liquid] | | |
| Gases | [gas] | | |
| Calibration sources: | ☐ | | |
| • Open source | ☐ | | |
| • Sealed source | ☐ [ISO standard] | | |
| • Isotope | | | |
| • Activity | | | |
| Use of activated material: | | | |
| • Description | ☐ | | |
| • Dose rate on contact and in 10 cm distance | [dose][mSV] | | |
| • Isotope | | | |
| • Activity | | | |
| **Non-ionizing radiation** | | | |
| Laser | | | |
| UV light | | | |
| Microwaves (300MHz-30 GHz) | | | |
| Radiofrequency (1-300 MHz) | | | |
| **Chemical** | | | |
| Toxic | [chemical agent], [quantity] | | |
| Harmful | [chem. agent], [quant.] | | |
| CMR (carcinogens, mutagens and substances toxic to reproduction) | [chem. agent], [quant.] | | |
| Corrosive | [chem. agent], [quant.] | | |
| Irritant | [chem. agent], [quant.] | | |
| Flammable | [chem. agent], [quant.] | | |
| Oxidizing | [chem. agent], [quant.] | | |
| Explosiveness | [chem. agent], [quant.] | | |
| Asphyxiant | [chem. agent], [quant.] | | |
| Dangerous for the environment | [chem. agent], [quant.] | | |
| **Mechanical** | | | |
| Physical impact or mechanical energy (moving parts) | [location] | | |

| | | | |
|---|---|---|---|
| Mechanical properties (Sharp, rough, slippery) | [location] | | |
| Vibration | [location] | | |
| Vehicles and Means of Transport | [location] | | |
| **Noise** | | | |
| Frequency | [frequency],[Hz] | | |
| Intensity | | | |
| **Physical** | | | |
| Confined spaces | [location] | | |
| High workplaces | [location] | | |
| Access to high workplaces | [location] | | |
| Obstructions in passageways | [location] | | |
| Manual handling | [location] | | |
| Poor ergonomics | [location] | | |

Hazard identification:

Average electrical power requirements (excluding fixed ISOLDE-installation mentioned above): [make a rough estimate of the total power consumption of the additional equipment used in the experiment]